# FINAL TECHNICAL REPORT

## Moored Observations of Nonlinear Internal Waves Near DongSha

## Performance Period: 1 March 2005 – 31 December 2009

Grant Number: N00014-05-1-0283

Matthew H. Alford, P.I.
Applied Physics Laboratory
*1013 NE 40th Street*
*Seattle, WA 98105*
phone: (206) 221-3257 fax: (206) 543-6785 email: malford@apl.washington.edu
http://faculty.washington.edu/malford/

**ABSTRACT**

Knowledge of internal waves and ocean mixing is important for advancing the performance of operational and climate models, as well as for understanding local problems such as pollutant dispersal and biological productivity. Nonlinear internal waves' (NLIWs) currents and displacements are strong enough to impact Navy operations such as diving, ROV operation and mine detection/removal. The South China Sea, where the internal waves are particularly strong, was selected as one of the field-study regions in part because of the excellent historical context provided by the ASIAEX experiment (Ramp et al, 2004). Dongsha Island (in the western South China Sea, Figure 1) was identified as a location where the propagation, transformation and dissipation of NLIWs could be tractably studied. An experiment was designed, moorings were deployed, and results were achieved and described within this report.

**WORK COMPLETED**

Wave arrivals and resultant speeds were computed for fourteen waves transiting the entire moored array. Speeds were compared to linear values computed from in-situ and climatological stratification. The data have been analyzed extensively, and compared to time series of barotropic tidal forcing at Luzon Strait. The work is in press at JPO.

In a separate effort with Jody Klymak, we are interested in understanding the energy and dissipation associated with the diurnal internal tide (as opposed to the nonlinear waves). Strong dissipation is observed there, as shown in past reports. Numerical modeling shows that a significant fraction of the energy is back-reflected at the shelf break, but that the forward-scattered portion can lead to internal hydraulic jumps and strong mixing in agreement with observations. The work has been submitted to JPO (Klymak first author).

| REPORT DOCUMENTATION PAGE | | | *Form Approved* *OMB No. 0704-0188* |
|---|---|---|---|



| 1. REPORT DATE *(DD-MM-YYYY)* | 2. REPORT TYPE | 3. DATES COVERED *(From - To)* |
|---|---|---|
| 14 - 05 - 2010 | FINAL TECHNICAL REPORT | 1 March 2005 – 31 December 2009 |

| | |
|---|---|
| 4. TITLE AND SUBTITLE<br>Moored Observations of Nonlinear Internal Waves Near DongSha | 5a. CONTRACT NUMBER |
| | 5b. GRANT NUMBER<br>N00014-05-1-0283 |
| | 5c. PROGRAM ELEMENT NUMBER |
| 6. AUTHOR(S)<br>Matthew Alford | 5d. PROJECT NUMBER |
| | 5e. TASK NUMBER |
| | 5f. WORK UNIT NUMBER |
| 7. PERFORMING ORGANIZATION NAME(S) AND ADDRESS(ES)<br>University of Washington, Applied Physics Laboratory<br>1013 N.E. 40th Street<br>Seattle, WA 98105 | 8. PERFORMING ORGANIZATION REPORT NUMBER |
| 9. SPONSORING/MONITORING AGENCY NAME(S) AND ADDRESS(ES)<br>Theresa Paluszkiwicz, Code 32<br>Office of Naval Research<br>875 North Randolph Street, Suite 1425<br>Arlington, VA 22203-1995 | 10. SPONSOR/MONITOR'S ACRONYM(S) |
| | 11. SPONSOR/MONITOR'S REPORT NUMBER(S) |

**12. DISTRIBUTION/AVAILABILITY STATEMENT**

UU

**13. SUPPLEMENTARY NOTES**

**14. ABSTRACT**

Knowledge of internal waves and ocean mixing is important for advancing the performance of operational and climate models, as well as for understanding local problems such as pollutant dispersal and biological productivity. Nonlinear internal waves' (NLIWs) currents and displacements are strong enough to impact Navy operations such as diving, ROV operation and mine detection/removal. The South China Sea, where the internal waves are particularly strong, was selected as one of the field-study regions in part because of the excellent historical context provided by the ASIAEX experiment (Ramp et al, 2004). Dongsha Island was identified as a location where the propagation, transformation and dissipation of NLIWs could be tractably studied. An experiment was designed, moorings were deployed, and results were achieved and described within this report.

**15. SUBJECT TERMS**

| 16. SECURITY CLASSIFICATION OF: | | | 17. LIMITATION OF ABSTRACT | 18. NUMBER OF PAGES | 19a. NAME OF RESPONSIBLE PERSON |
|---|---|---|---|---|---|
| a. REPORT | b. ABSTRACT | c. THIS PAGE | | | Leslie Harding |
| UU | UU | UU | unlimited | 1 | 19b. TELEPHONE NUMBER *(Include area code)*<br>206-543-7048 |

Reset

**Standard Form 298** (Rev. 8/98)
Prescribed by ANSI Std. Z39.18

## RESULTS

1. A set of fourteen waves was tracked nearly across the entire basin (Figure 3a). As found by Ramp et al (2004), larger waves alternate with smaller ones, termed ‘A’ and ‘B’ waves, respectively. Tracking back to the Luzon Strait eastern ridge assuming travel at the semidiurnal mode-1 speed, their generation time is compared to measured and TPXO model-predicted tidal currents there (b, c). Waves appear to be generated at or somewhat after maximum eastward tidal currents, as suggested by several numerical models (e.g. Buijsman, 2009). This contrasts with the findings of Zhao and Alford (2006), who did not have data in the deep basin. However, this result is complicated by a lack of data in the true nearfield. We aim to remedy this situation in the ongoing IWISE DRI, which seeks to focus on generation at Luzon Strait’s two ridges.

2. Their speeds were computed by differencing arrival time pairs (Figure 3b), and compared to linear values (3b,c). Speeds are ~10-20% in excess of semidiurnal linear values for all but the smallest waves in the deep basin.

3. Larger ‘A’ waves travel faster than small ones in the deep basin, but the reverse holds true in the shallower water to the west. This is shown to be due to the effect of the diurnal internal tide on the wave speed there. Since the waves arrive twice daily, every other wave opposes the baroclinic flow of the once-daily diurnal internal tide (Figure 4, bottom), which slows the wave speed. Solutions of the Taylor-Goldstein equation give predictions of the correct magnitude and sign as observed. These findings highlight the need to know the background currents in order to accurately predict speed and arrival time, particularly in shallow water where the wave speeds are comparable to the background flows.

4. Significant reflection of the diurnal internal tide is seen, together with large dissipation values (Figure 5). By contrast, the semidiurnal tide shows little reflection. A linear model reproduces this behavior well.

## REFERENCES

Alford, M. H., R. Lien, H. Simmons, J. M. Klymak, Y. Yang, D. Tang, and M. Huei Chang. Speed and evolution of nonlinear internal waves transiting the South China Sea. J. Phys. Ocean., submitted:1–20,
2010.

Buijsman, M.C, Y. Kanarska, and J. C. McWilliams. On the generation and evolution of nonlinear internal waves in the South China Sea. J. Geophys. Res., in press, 2009.

Ramp, S. R., D. Tang, T. F. Duda, J. F. Lynch, A. K. Liu, C. S. Chiu, F. Bahr, Y. R. Kim, and Y. J. Yang, Internal solitons in the northeastern South China Sea, part I: sources and deep water propagation, IEEE J. of Oceanic Engr., 2004.

Zhao, Z., and M. H. Alford, Source and propagation of nonlinear internal waves in the northeastern South China Sea, J. Geophys. Res., 111, doi:10.1029/2006JC003,644, 2006.

**PUBLICATIONS**

M. H. Alford, R. Lien, H. Simmons, J. M. Klymak, Y. Yang, D. Tang, and M. Huei Chang. Speed and evolution of nonlinear internal waves transiting the South China Sea. *J. Phys. Ocean.*, in press: 1–20, 2010.

A manuscript describing the work with Klymak has just been submitted to JPO (Klymak first author).

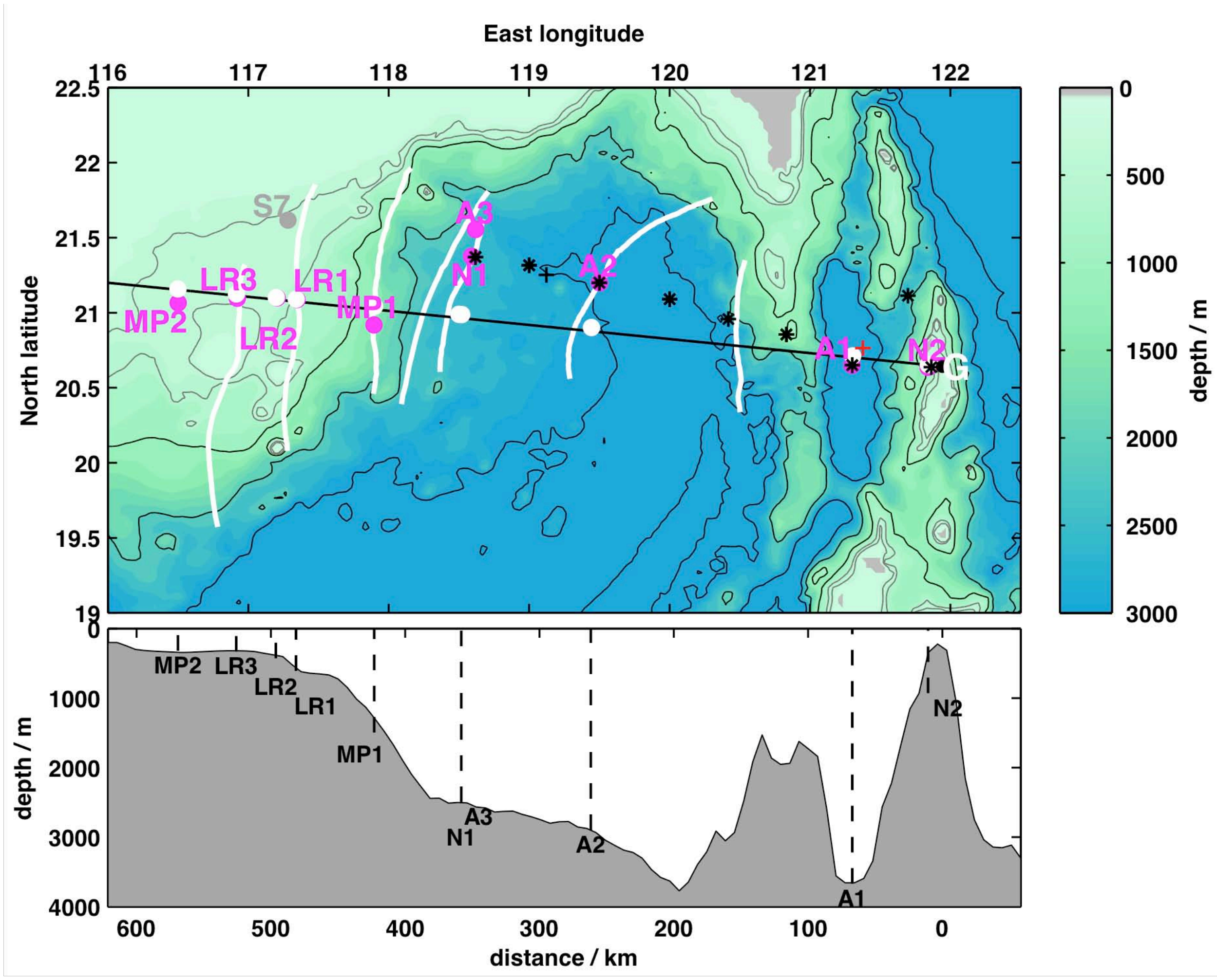


***Figure 1: Map of study region showing depth (colors), mooring locations (magenta), the propagation track assumed in calculating wave speed (black line), the assumed generation site ("G"), and the location of each mooring projected onto it assuming cylindrical spreading (white; see text). Selected NLIW crests from 1998-2001 from SAR radar (courtesy of Z. Zhao) are shown in white. Asterisks and pluses indicate the locations of CTD casts used to compute linear phase speeds. Bottom panel shows bathymetry along the track.***

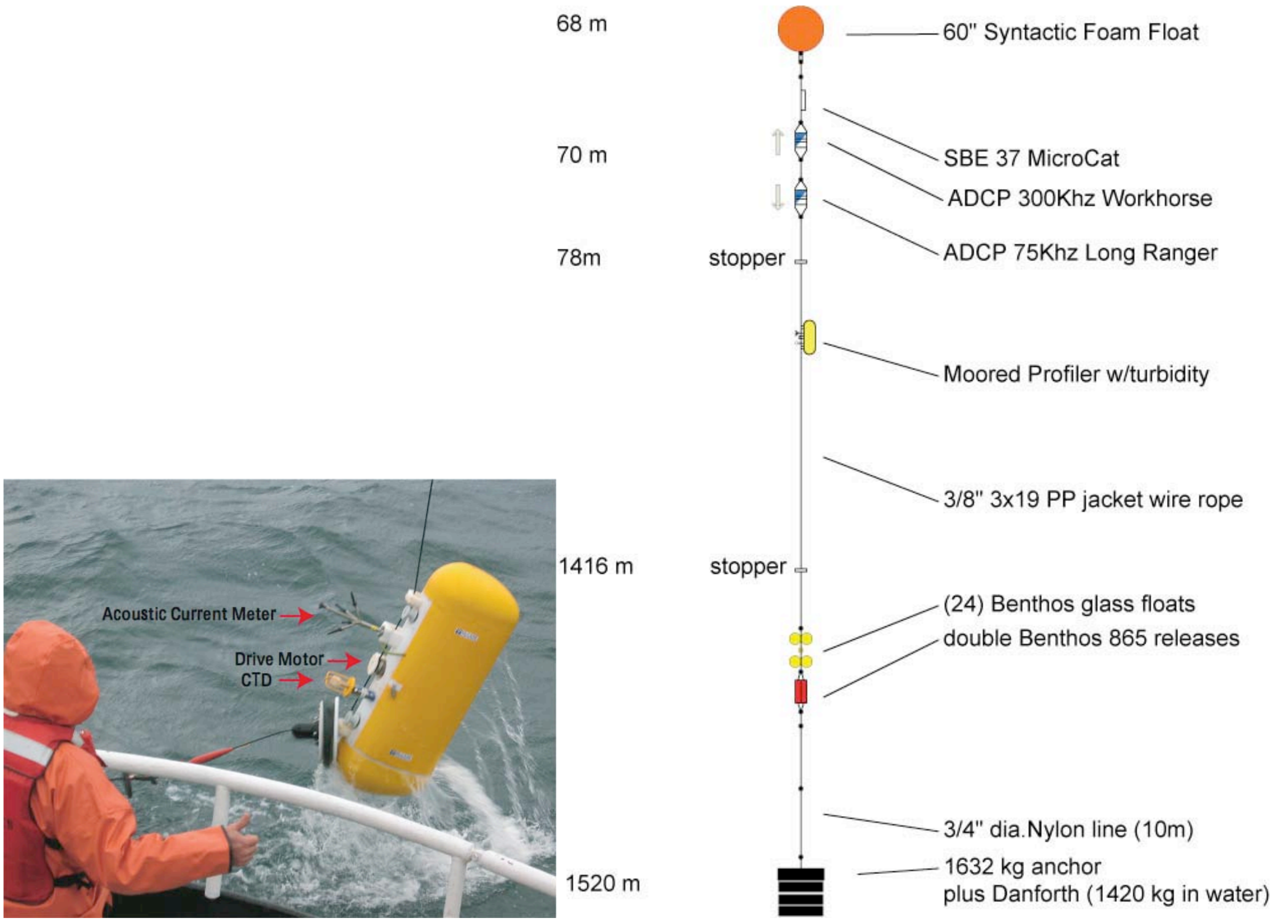


***Figure 2: (Left) The McLane Moored Profiler being recovered in Puget Sound, WA. (Right) Mooring diagram at MP1. The uplooking ADCP did not function owing to a failed memory card. The shallow mooring at MP2 (not shown) is similar, with the MP sampling the range 60-300 m in 320 m of water.***

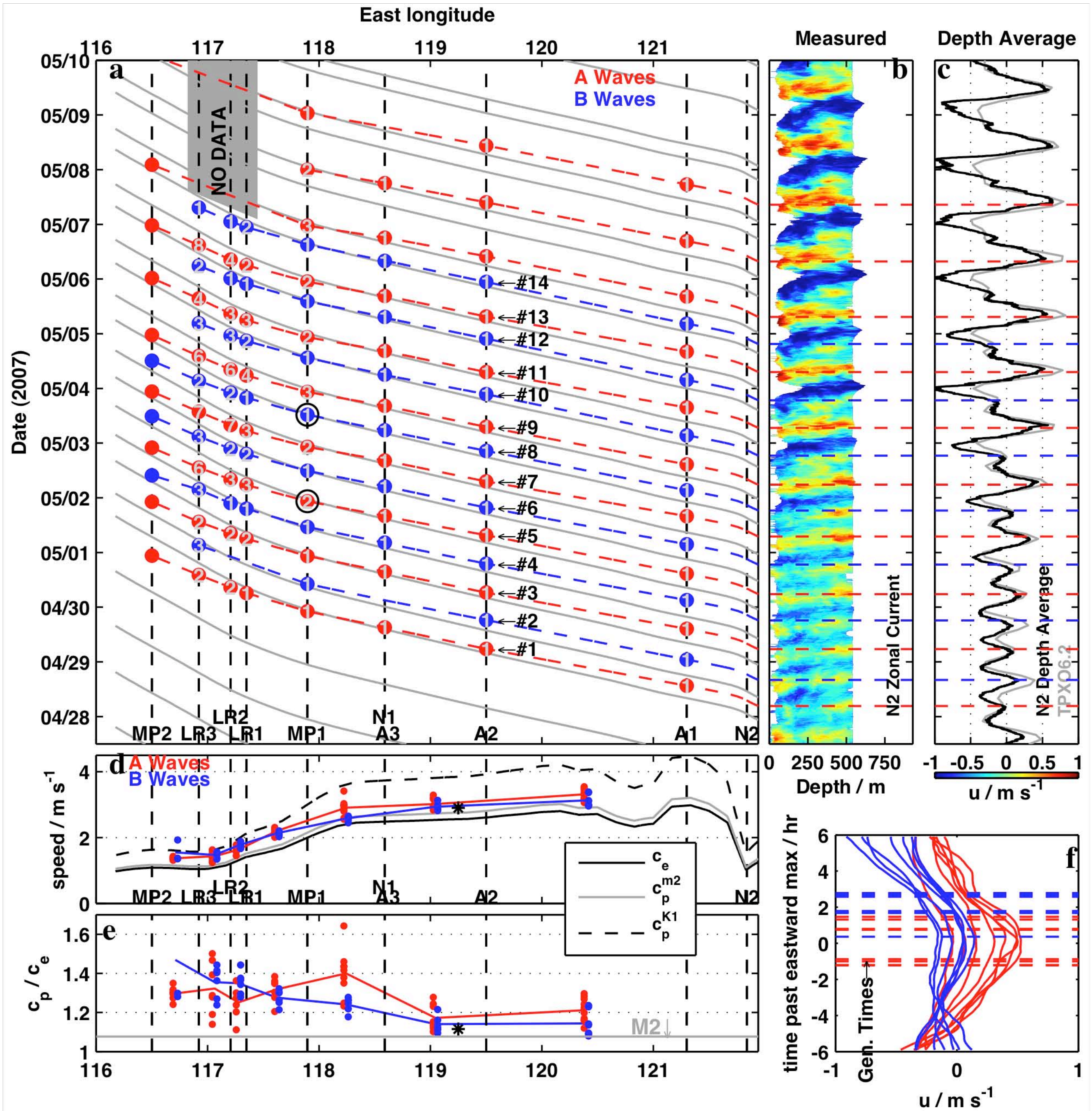


*Figure 3: Summary of all detected wave arrivals and corresponding speed. (a) Arrival times of A and B waves (red and blue dots). White numbers indicate the number of waves in the train (1 indicating a single wave). Red/blue dashed lines are the interpolated observed arrivals, with the linear semidiurnal phase speed used to extrapolate east of A1. The right plotting limit is the assumed generation site. Gray lines are trajectories beginning at westward current maxima at Luzon Strait and traveling at the linear irrotational phase speed. (b) Zonal barotropic currents at Luzon Strait predicted from TPXO6.2 (gray) and depth-averaged zonal currents measured at N2 (black). The depth-dependent currents are contoured versus depth and time in (c). The right axis limit is the water depth, and the color bar is shown below (b). Dashed lines in (b, c) indicate generation times determined from the intercept of the extrapolated trajectories in (a). (d) Speed*

***along the track in Figure 1 determined from differential arrival times for A waves (red dots) and B waves (blue dots), plotted slightly to the left/right of the mooring location for visibility, and the mean over all A and B waves (red and blue line, respectively). (red line) and B waves (blue line). Linear long-wave speeds for waves with no rotation (black), semidiurnal waves (gray) and K1 (dashed) are overplotted. (e) The ratio of observed speed to irrotational linear speed for A and B waves (red and blue dots), and their mean (lines). The ratio for semidiurnal waves is shown in gray. (f) Generation time (horizontal dashed lines) and depth-average current at N2 (solid) for A and B waves (red and blue, respectively). Time is relative to that of maximum eastward flow.***

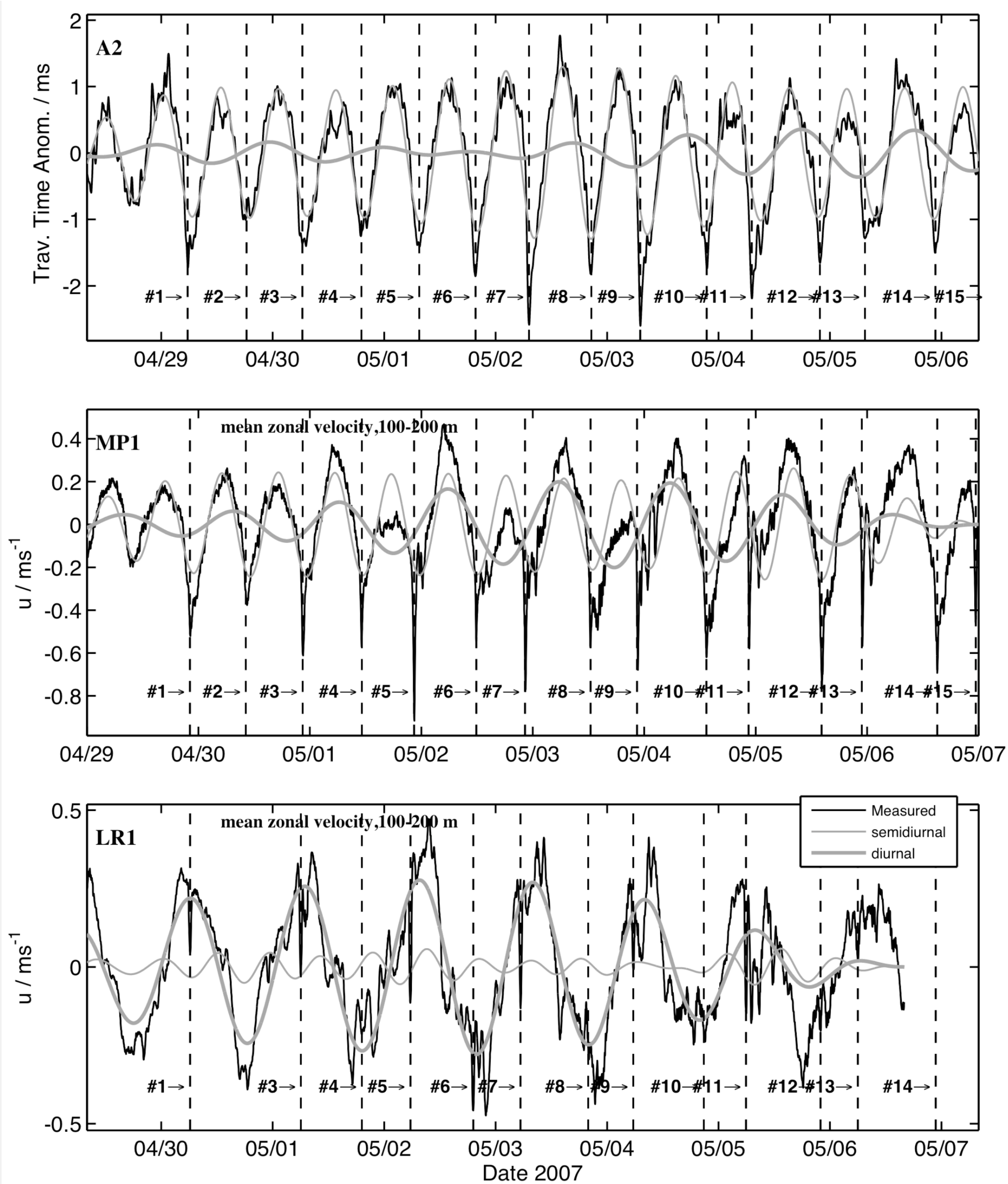


*Figure 4: (a) Total (black), semidiurnal (light gray), and diurnal (heavy gray) travel time anomaly at A2. (b,c) As (a) but for zonal current averaged between 100-200 m at MP1 (b) and LR1 (c). Wave arrivals are indicated. Each panel is lagged for mean travel time.*

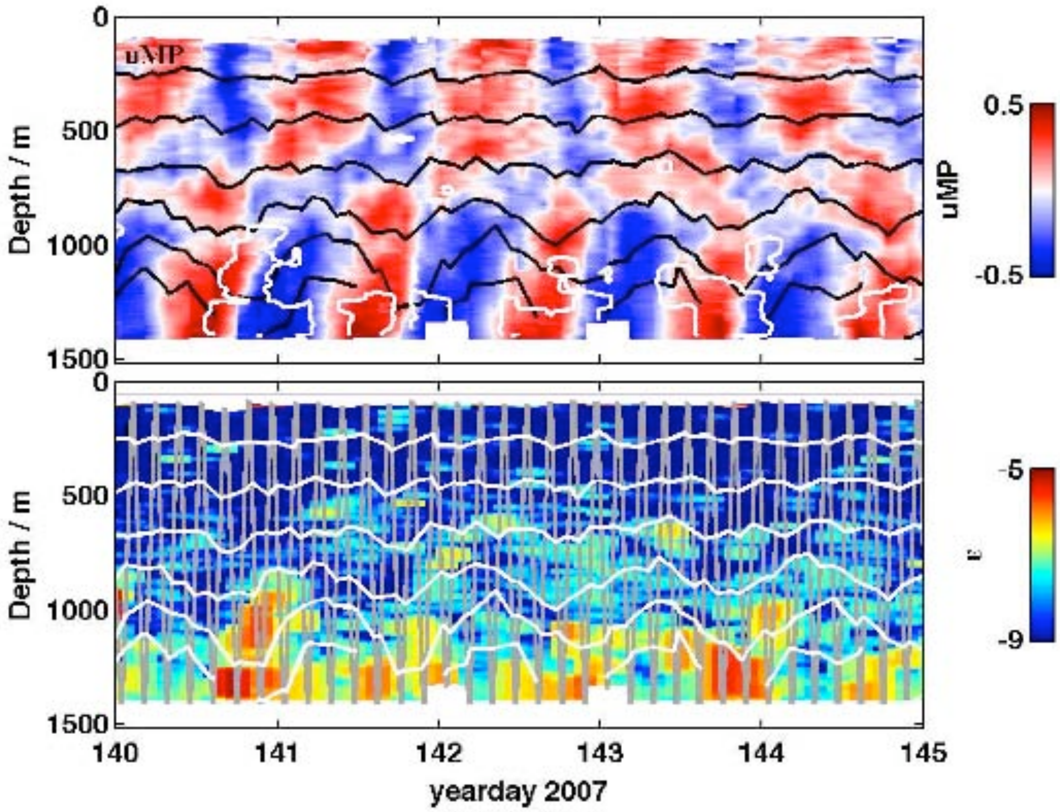


***Figure 4: Velocity (top) and dissipation rate, (bottom) measured with the MP over a 5-day period during a spring tide. Isopycnals are overlaid. Regions of $\varepsilon > 10^{-6.5}$ Wkg$^{-1}$ are outlined in white. Strong dissipations occur owing to strain events associated with diurnal internal tide motions on the sloping bottom. The moored profiler track (bottom, gray) indicates that these motions are well resolved.***